9 Low-Temperature Thermometry

Contents

9.1 Introduction

A thermometer is a device by which we can measure a property of matter function of temperature. If a relation, based on fundamental laws of physics, between such property and the thermodynamic temperature is considered reliable, the thermometer does not need a calibration and is called *primary thermometer*. In the other cases, the thermometer needs a calibration and is called *secondary*. Examples of primary thermometers are gas thermometers and noise thermometers.

Primary thermometry is usually quite difficult and reserved to metrological laboratories.

Secondary thermometers must be calibrated by means of a primary thermometer or at fixed points as discussed in Chapter 8. Secondary thermometers are often quite easy to use and more sensitive than primary thermometers. A typical example of secondary thermometer is the electrical resistance thermometer (see Section 9.6).

Table 9.1
Common low-temperature thermometry

1	Gas thermometry
2	Vapour pressure thermometry
3	^{3}He melting pressure thermometry
4	Thermoelectric power thermometry
5	Resistance thermometry
6	Noise thermometry
7	Dielectric constant thermometry
8	Electronic paramagnet thermometry
9	Nuclear paramagnet thermometry (range 1–100 μK)
10	Nuclear orientation thermometry
11	Coulomb blockade thermometry

In most cases, one thermometer is useful only in a limited temperature range. Usually, out of the useful range, it simply loses sensitivity: for example a Pt thermometer (see Section 9.6.1) shows an electrical resistance which decreases of ∼0.13%/K down to ∼20 K, but only of ∼0.01%/K at 10 mK.

A good low-temperature thermometer should possess several qualities:

- reproducibility and high sensitivity;
- wide operating range and low sensitivity to environmental changes such as magnetic or stray fields;
- short time to reach equilibrium and fast reading system. A low heat capacity of the sensor is not sufficient to obtain fast readings of temperature (see Section 9.11);
- at very low temperature, the heat introduced by the measurement must be as low as possible to avoid overheating of the sensor (see Section 9.5).

Since most of the properties of materials depend on temperature, there are a lot of possible choices for a thermometer. Some thermometric properties like Mössbauer effect or osmotic pressure, of historical interest, but no longer in use, are reported in ref. [[1], pp. 200–206]. Hereafter, some thermometric properties useful at low temperature are described (see Table 9.1). Due to the enormous amount of papers on the subject, the bibliography cannot be complete. References before 1980 are reported in ref. [2].

Useful source of information about thermometry are ref. [3–8].

9.2 Gas thermometry

The three modern types of gas thermometry – constant volume gas thermometry (CVGT), acoustic gas thermometry (AGT) and dielectric constant gas thermometry (DCGT) – are presently considered ‘primary’. They are based on simple relations between the properties of an ideal gas and temperature T. However, the departure from the ideal behaviour must be carefully considered in view of the desired level of accuracy. This is done by measuring the thermometric property as a function of density. Then the ideal

behaviour is deduced by fitting an appropriate expansion to the measured isotherm and extrapolating to zero density. We wish to remark the fact that AGT and DCGT are based on the variation with T of an intensive property of the gas (speed of sound and dielectric constant, respectively), whereas primary CVGT requires the knowledge of the number of moles of gas present in the gas bulb.

9.2.1 Constant volume gas thermometry (CVGT)

In the CVGT, the pressure in a fixed amount of gas is related to the temperature using an equation of state for the gas in the form:

$$pV = nRT \cdot \left[1 + B(T) \cdot n/V + C(T) \cdot (n/V)^2\right] \tag{9.1}$$

where $n =$ moles of gas in the volume V.

At low temperature, in eq. (9.1) only the coefficient B is significant [3], whereas at very low temperature also C must be taken into account. Values of the coefficients for ^{3}He and ^{4}He are reported in ref. [9–14].

The filling gas pressure of a CVGT must be carefully chosen: it must be high enough to get a good sensitivity and low enough to approximate the ideal gas behaviour.

The accuracy in the measurement of pressure p depends on the lowest temperature down to which the CVGT is used. For example, with an allowed pressure variation $\Delta p = 0.133\,\text{Pa}$, the minimum allowed temperature is $\approx 2\,\text{K}$ for ^{4}He and $\approx 1\,\text{K}$ for ^{3}He respectively. With a fixed number of moles N, the CVGT gives T carrying out two pressure measurements: at the temperature T to be determined and at a known temperature $T_{\text{ref.}}$. The requirements for the constancy (practically the knowledge) of N in a CVGT are the following:

(a) Dead volume (manometers, valves and capillary tube connecting the pressure gage) should be small and possibly constant (e.g. the amount of gas in the dead volume, such as the capillary, depends also on the temperature distribution and hence on the reproducibility of the gradient along the capillary), since corrections for their contribution are to be taken into account;
(b) Thermal and elastic volume changes (as a function of T) of various components (e.g. the gas bulb) of the CVGT should be known;
(c) Adsorption and desorption of gas from the walls should be evaluated. To minimize these phenomena, helium is the most favourable gas, since its chemical adsorption is negligible and its adsorption energy is the lowest among noble gases. Nevertheless, it is worth reminding that desorption is an irreproducible phenomenon because it depends not only on temperature but on the previous 'thermal history' of the device;
(d) Impurities (usually H_2 in ^{4}He and ^{4}He in ^{3}He) in the gas change the value of B in eq. (9.1);
(e) The 'aerostatic head' must be considered (see ref. [15]): it is defined as the pressure difference Δp due to a gas column of height h and density $\rho(T)$. Δp is proportional to $1/T$. The effect is mainly due to the low-temperature region, i.e. the bulb itself. Hence the aerostatic head correction depends on the bulb temperature T;

(f) Thermomolecular pressure difference along the capillary connecting the bulb to the room temperature gage (see e.g. ref. [16]);
(g) A low-temperature pressure gage, of course, eliminates or minimizes many of the aforementioned problems (see e.g. ref. [17]). Note that it must stand the room temperature gas pressure in the bulb.

The realization of a CVGT with a high level of accuracy requires complex techniques and skill. It is mostly used by national laboratories for calibration purposes. For a detailed description of CVGT, see e.g. ref. [18].

Over the years, a simpler instrument called 'interpolating constant volume gas thermometer' (ICVGT) has been developed. It differs from traditional CVGT because it is calibrated at a number of temperatures known from independent measurements.

In the ITS-90, the ICVGT has been introduced instead of the CVGT for its simplicity and better reproducibility. By means of the ICVGT, temperatures are defined in the range from 3 K to the triple point of Ne (24.5561 K) by interpolating curves (established according to an international agreement) referring to ^{3}He or ^{4}He gas pressure [19–21]. Suppose that everything is in the same situation both during calibration and measurement (e.g. the same thermal distribution in the capillary), by means of the calibration at fixed points of the ICVGT, the corrections listed before ((a) through (f)) are not needed. In particular the p used in the interpolating formula is the pressure measured by the manometer and not the pressure inside the bulb.

In the ICVGT, corrections (a), (e) and (f) are not taken into account. When using the established quadratic interpolation curve, these corrections (within 0.3 mK) are taken into account through the factor B of eq. (9.1). Details of construction and operation for ^{3}He and ^{4}He ICVGT are reported in ref. [22,23] for ^{3}He and [24–26] for ^{4}He.

The problems encountered in performing accurate measurements of T with a primary CVGT can be overcome by the use of the dielectric constant gas thermometer [27–31] or by the acoustic gas thermometer [3,32,33].

9.2.2 Acoustic gas thermometry (AGT)

Sound waves are propagated in a gas as longitudinal waves of speed v_s:

$$v_s = \left(B_S/\rho\right)^{1/2} \tag{9.2}$$

where B_S is the adiabatic bulk modulus and ρ the gas density.

For an ideal gas:

$$v_s = \left(\gamma \cdot RT/M\right)^{1/2} \tag{9.3}$$

with M the molar mass and $\gamma = C_P/C_V$ ratio. Corrections are small except at very low temperatures. Difficulties or errors have been nevertheless encountered because of the propagation of higher frequency modes or boundary effects. Descriptions of the NIST and NPL acoustic thermometers can be found in ref. [3]. Details of a spherical interferometer giving uncertainties below 0.3 mK can be found in ref. [32–34].

9.2.3 Dielectric constant gas thermometry (DCGT)

The basic idea of DCGT is to replace the density in the state equation of a gas by the dielectric constant ε.

For an ideal gas, this yields the simple relation between the pressure p and ε:

$$p = k_B T \cdot (\varepsilon - \varepsilon_0) / a_0 \tag{9.4}$$

where ε_0 is the exactly known vacuum dielectric constant and a_0 the static electric dipole polarizability of a gas atom (see Fig. 9.1). The measurement of DCGT isotherms yields A_ε / R and thus:

$$k_B = \left(R / A_\varepsilon\right) \cdot a_0 / (3\varepsilon_0) \tag{9.5}$$

where A_ε is the molar polarizability.

As AGT, DCGT avoids the troublesome density determination of the conventional gas thermometry. In addition, the pressure sensing tubes can be of any convenient size, and the thermometric gas can be moved in or out the bulb without the need to allow for the amount of the gas involved.

Absolute DCGT requires knowing a_0 with the necessary accuracy. Nowadays this condition is fulfilled for helium. Recent progress has decreased the uncertainty of the value of a_0 well below 10^{-6} [35,36]. Up to now, DCGT using cylindrical capacitors for

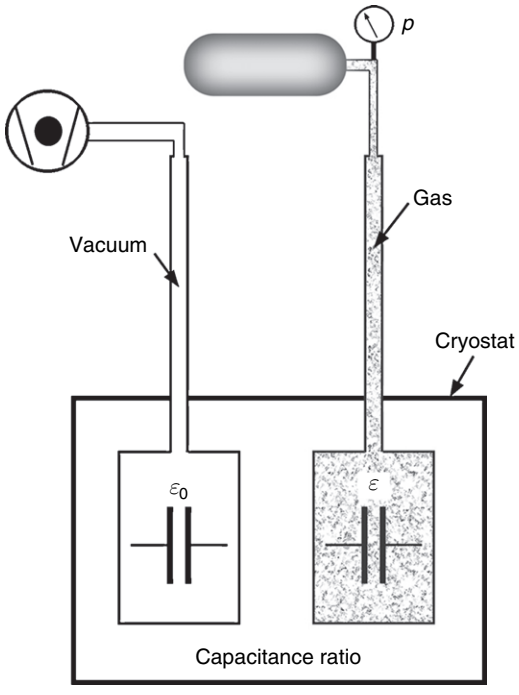

Fig. 9.1. Schematics of dielectric constant gas thermometry.

determining ε has been performed by two groups in the range from about 3 to 27 K [37,38]. The obtained relative uncertainties are of order of 10^{-5}, but it seems to be possible to decrease the uncertainty at least by an order of magnitude by optimizing the capacitor design and with in situ measurements [39].

Further progress depends essentially on the developments in p and C measurements. A new proposal is to apply quasi-spherical resonators for DCGT [40].

9.3 Vapour pressure thermometry

The vapour pressure of a liquid depends on the kind of liquid and changes rapidly with temperature (see Section 2.4). Hence, there is the possibility of realizing convenient secondary thermometers, which were widely used before the advent of commercially calibrated resistance thermometers.

From eq. (2.3) of Section 2.2.4.1, the vapour pressure over a liquid (with latent heat of evaporation $L = \text{constant}$) can be written as:

$$\ln(p) = \frac{A}{T} + B \tag{9.6}$$

However, in reality, $L = L(T)$; hence an empirical equation is commonly used:

$$\ln\left(\frac{p}{p_0}\right) = a + \frac{b}{T} + c \cdot T + \ldots \tag{9.7}$$

A compilation of the vapour pressure of various liquids can be found in ref. [41].

The most interesting liquids for low-temperature thermometry are ^{3}He and ^{4}He, especially for the calibration of resistance thermometers in the range from 0.5 to 4.2 K. Vapour pressure of H_2 is also interesting to realize vapour pressure-fixed points included in ITS-90. The measure of He vapour pressure has been carried out with great accuracy [42,43] to establish the ITS-90 (see Section 8.3). There are several experimental precautions to be observed in order to obtain reliable measurements [2].

Also in the vapour pressure thermometer, the presence of impurities, isotopes or different spin states must be evidenced and minimized.

The main problem encountered in the realization of a vapour pressure thermometer is the correct measurement of the pressure p. In this case, however, the dead space is not a problem and larger tubes may be used (instead of capillaries). Since the pressure gage is usually at room temperature, also in this case, a gradient in temperature between the cold and the warm end of the sampling tube produces a thermomolecular pressure difference [44,45, p. 48]:

$$\frac{\mathrm{d}p}{\mathrm{d}T} = \frac{p}{2T} \cdot f\left(r/\lambda\right) \tag{9.8}$$

where r is the radius of the tube, λ is the mean free path of the gas particles and f is a function of the ratio r/λ.

Thermomolecular pressure difference is present in vapour pressure with any gas. In the case of ^{4}He, additional problems occur: above the lambda point (see Section 2.2.4.1), the result is that the temperature above the surface may be a few millikelvin lower than that

of the liquid. These effects can be reduced by containing the liquid in a high-conductivity chamber. Below lambda point, He II is a very good heat conductor so that temperature gradients do not exist in the liquid. Anyway, the flow of a superfluid He film creeping to the warmer part of the tube wall may be a problem: this steady heat flow into the container gives raise to a temperature difference between the liquid and the walls of the container, accentuated by the presence of a Kapitza resistance at the solid–liquid interface. Temperature gradients can only occur in the case of liquid ^{3}He which is a poor heat conductor.

A detailed discussion of the problems encountered in vapour pressure measurements at low temperature is given in ref. [46,47], where also the use of an 'in situ' manometer is described. Vapour pressure gas thermometry with other liquids besides He is discussed in ref. [43, p. 49].

9.4 ^{3}He melting curve thermometry

As we saw in Chapter 7, the ^{3}He melting curve, shown in Fig. 7.1, is described by the Clausius–Clapeyron equation:

$$\left(\frac{\mathrm{d}p_f}{\mathrm{d}T}\right)_{\text{vap.}} = \frac{S_{\text{liq.}} - S_{\text{sol.}}}{V_{\text{m,liq.}} - V_{\text{m,sol.}}} \tag{9.9}$$

where f refers to fusion.

Since the liquid molar volume is always larger than that of solid [48,49], $\mathrm{d}p/\mathrm{d}T < 0$ if $S_{\text{liq.}} < S_{\text{sol.}}$.

For temperatures above 0.32 K, the entropy of liquid is higher than that of the solid as happens in all other materials (see Section 7.2.1); below 0.32 K, the situation is reversed. We remind that this property allows to cool the liquid by isoentropic compression (see Section 7.1).

To use the ^{3}He melting pressure as thermometric property, pressure is measured in situ by means of capacitance pressure gage [50]. With a pressure resolution of 10 microbar, the precision in the measurement of temperature is 3×10^{-4} at 1 mK, 3×10^{-5} at 10 mK and 5.10^{-6} at 100 mK [51].

The confidence in the theoretical relationship between pressure and temperature along the melting curve led to state as primary this type of thermometer and put it as the base of PLTS 2000 down to 0.9 mK (see Section 8.5).

For the realization of a primary melting curve thermometer (MCT), three different methods have been suggested and tested:

1. From the knowledge of the quantities (known by independent measurements) in Clausius–Clapeyron equation, the slope of the fusion curve can be evaluated and integrated to get $p_f(T)$. For example, in the 5–20 mK range, the Clausius–Clapeyron equation gave temperature values with an 1% accuracy [52,53];
2. From the temperature T defined as:

$$T = \frac{\mathrm{d}Q}{\mathrm{d}S} = \left(\frac{\mathrm{d}Q}{\mathrm{d}p_f}\right) \cdot \left(\frac{\mathrm{d}p_f}{\mathrm{d}S}\right) \tag{9.10}$$

where $\mathrm{d}Q/\mathrm{d}p_f$ is the measured $\mathrm{d}Q$ needed to produce a pressure change $\mathrm{d}p_f$. Instead, $\mathrm{d}p_f/\mathrm{d}S$ can be evaluated from a series of thermodynamic transformation [52,54];

3. The third method is a variation of the second: a heat pulse $\mathrm{d}Q$ is supplied, keeping both the pressure and temperature constant by means of a feedback system. In this process, some moles of liquid ^{3}He are solidified: the latent heat of solidification is the measured $\mathrm{d}Q$. Since from Clapeyron equation:

$$\frac{\mathrm{d}p_f}{\mathrm{d}T} = \frac{\mathrm{d}S}{\mathrm{d}V} \tag{9.11}$$

from $\mathrm{d}Q = T\mathrm{d}S$, we get:

$$\frac{\mathrm{d}Q}{\mathrm{d}V} = T \cdot \frac{\mathrm{d}p_f}{\mathrm{d}T} \tag{9.12}$$

By measuring $\mathrm{d}Q/\mathrm{d}V$ for some pressure values along the melting curve, by integration, we get:

$$T = \overline{T} \times \exp\left(\int_0^{p-\overline{p}} \left(\mathrm{d}V/\mathrm{d}Q\right) \mathrm{d}p' \right) \tag{9.13}$$

where p' is the pressure difference measured along the melting curve with a fixed point $\overline{p}$. Integration of eq. (9.13) gives the temperature from the knowledge of one fixed point $\overline{T}$.

The method, developed at Cornell for the 1–25 mK, allows one to get T without the knowledge of $\overline{T}$. In fact, all the quantities which describe the system can be evaluated as functions of the ratio $T/\overline{T}$. On the other hand, $\overline{T}$ can be evaluated at the end as a fit parameter [55].

Even if nowadays, the MCT may be considered a primary thermometer only on a narrow temperature range, it is considered the best dissemination standard in the millikelvin range [56–59]. In fact, the ^{3}He melting pressure is a good thermometric property because of its sensitivity over three decades of temperature with a resolution $\Delta T/T$ up to 10^{-5} [56]. The good repeatability, the insensitivity to magnetic fields up to 0.5 T [60] and the presence of temperature-fixed points allow for the control of possible shifts in the calibration curve of the pressure transducer. The usefulness of these fixed points is evident, considering that the ITS-90 is based just on the definition of fixed points.

The precautions in a thermometric measurement with the ^{3}He melting curve thermometer are the control of the impurity from ^{4}He [61] and of presence of high magnetic fields [62,63].

The advantages of this thermometer are the high resolution (about 1 μK), repeatability (a few ppm), the zero power dissipation and the insensitivity to radio frequency (RF) fields. The experimental realization is however quite complicated.

9.5 Thermocouples

The use of the thermoelectric power of metallic junctions presents the following advantages:

- it is a local measurement with point sensors;
- the apparatus is simple and the measurements are quite easy;

- the thermometer is usually insensitive to magnetic fields;
- the sensors have low heat capacity;
- no power is involved in the measurement;
- measurements are reproducible.

Unfortunately, the thermoelectric power vanishes when temperature tends to zero: pairs as the classic Cu/constantan thermocouples show very low sensitivity below 10 K (see Fig. 9.2).

However, new materials have been found which allow the extension of the measurements to the millikelvin region. These materials contain a small amount of magnetic dopants as Au/Fe or Pd/Fe, see Fig. 9.3 [64].

Obviously, the small thermoelectric powers produced by metal pairs at low temperatures cannot be measured using a reference temperature of 0°C, where the thermoelectric power is high; a 4.2 K bath is a typical reference.

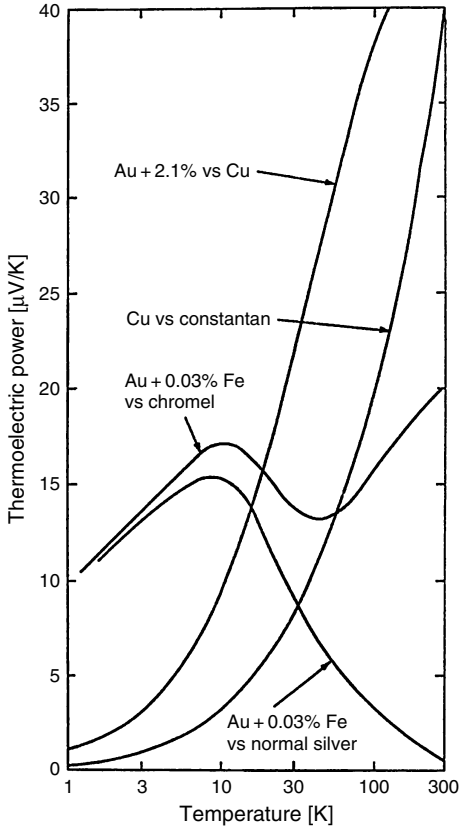

Fig. 9.2. Thermometric power of some metal pairs at low temperature [19].

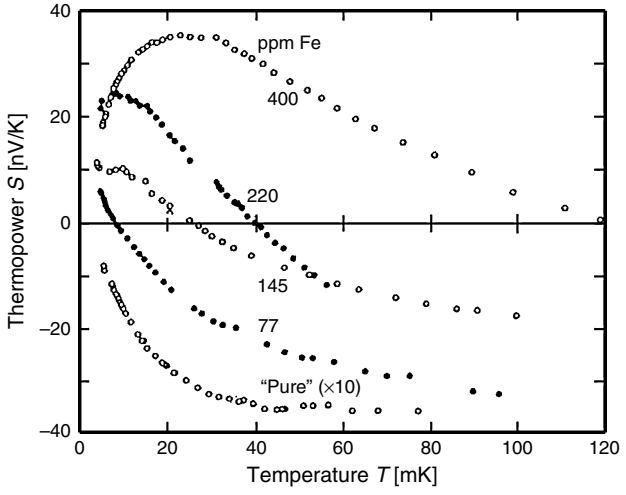

Fig. 9.3. Thermoelectric power of Pd doped with Fe (in ppm) as a function of temperature. The value for the pure sample has been multiplied by 10 for sake of clarity [64].

The main drawback in this type of thermometry is the presence of spurious thermoelectric powers due to chemical inhomogeneity, stress in conductors, contact effects in switches if present, etc.

The measurements are carried out with an a.c. bridge or with a SQUID at the lower temperatures. The resolution is of the order of 1 μK at 1K.

9.6 Resistance thermometry

The resistance thermometry is based on the temperature dependence of the electric resistance of metals, semiconductors and other resistive materials. This is the most diffused type of low-temperature thermometry: sensors are usually commercial low-cost components. At very low temperatures, however, several drawbacks take place such as the low thermal conductivity in the bulk of the resistance and at the contact surface, the heating due to RF pick up and overheating (see Section 9.6.3)

Laws describing the resistance–temperature dependence are not reliable: hence resistance thermometers are secondary devices.

9.6.1 Metal thermistors

The electric resistance of metals decreases as temperature is lowered down to about 20 K. The most used metal as thermometric material is platinum. Platinum is chemically resistant and can be produced with high purity (minimizing the temperature-independent

Table 9.2
Temperature-resistance values for a Pt-100 thermometer

Temperature [K]	Resistance [Ω]
10	0.09
15	0.19
20	0.44
25	0.94
30	1.73
40	4.18
50	7.54
60	11.45
77	18.65
100	28.63
125	39.33
150	49.85
175	60.23
200	70.50
225	80.66
250	90.72
273.2	100.00
300	110.63

contribution to resistivity = high RRR); it is ductile, hence can be drawn in thin wires, and finally its resistivity temperature coefficient is quite high.

The commercial Pt series resistance are well known. The characteristic of Pt-100 resistor are reported in Table 9.2 and Fig. 9.4.

It is important that the metal wire is strain free so it does not change its properties on repeated thermal cycles.

As we said, the sensitivity of a metallic thermometer drastically falls below about 10 K; as it was the case of the thermoelectric power; it is possible to increase the sensitivity by introducing some magnetic impurities. The most commonly used magnetic alloy is the commercial Rh-0.5% Fe (see Fig. 9.5).

9.6.2 Semiconductors, carbon and metal oxide thermistors

We can notice in Fig. 9.5 that Pt and Rh-Fe thermometers have a positive temperature coefficient, whereas other reported materials have a negative coefficient. They usually are either semiconducting or amorphous materials.

The formula which approximately describes the $R(T)$ dependence is the Mott's law [65]:

$$R = R_0 \cdot \exp\left(\frac{T_0}{T}\right)^n \tag{9.14}$$

where n ranges between 0.25 and 0.6 and T_0 between ∼1 and ∼100 K (see Section 15.2.1).

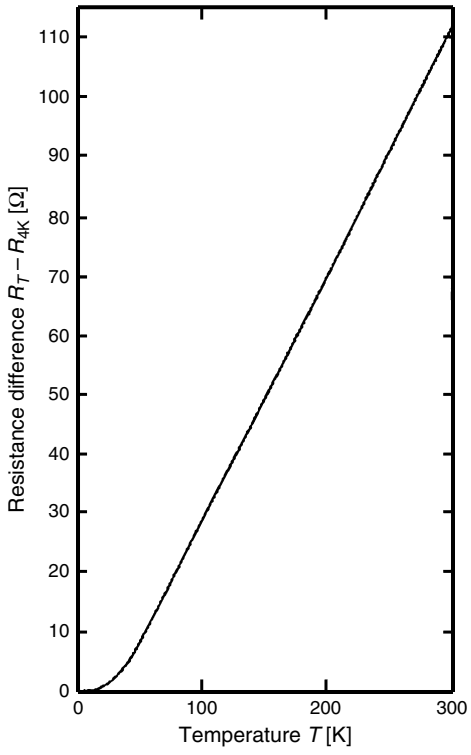

Fig. 9.4. Difference of resistance of Pt at the temperature T and at 4.2 K versus temperature. The curve is linear down to 50 K (data from [19]).

9.6.2.1 Doped germanium resistors

Germanium used for thermometric purposed has doping values of 10^{15}–10^{19} atoms/cm^3. Classic doping methods do not lead to the best results for Ge. In order to obtain a high-doping homogeneity, the so-called NTD (neutron transmutation doping) is used: pure Ge is irradiated by a flux of thermal neutrons produced by a nuclear reactor. Neutrons are captured by some lattice atoms which are transmutated into atoms of the third group. This process (see Section 15.2.1.1) produces a *p*-type doped Ge.

A precious quality of Ge thermometers is their stability (better than 0.1% after repeated cooling cycles). Problems at very low temperatures are:

1. the electron–phonon decoupling (see Section 15.2.1.3);
2. an excess of noise (see ref. [66,67]);
3. high thermal resistance towards support; this means that measurements must be done with a very low power. This drawback is common to all other resistance thermometers.
4. a high magnetoresistance which depends on the orientation respect to the magnetic field and increases with the sensitivity of the thermometer (that is with T_0) [68,69],

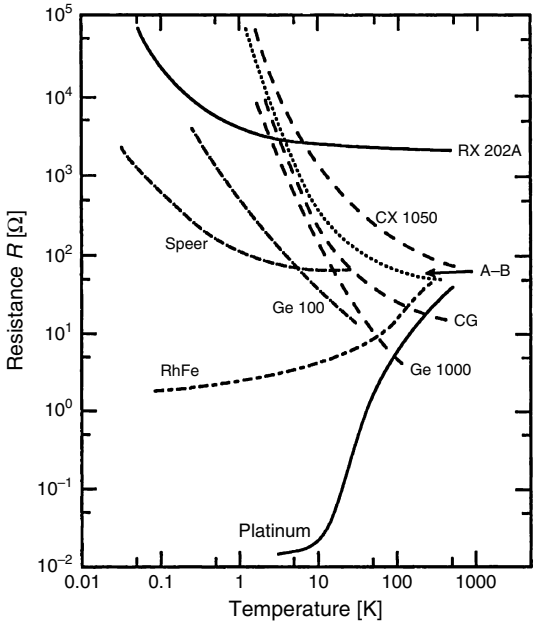

Fig. 9.5. The electrical resistance $R(T)$ for some typical thermometers. A–B denotes Allen–Bradley carbon resistor. Speer is a carbon resistor. CG is carbon-in-glass. CX 1050 is a Cernox and RX 202A is a ruthenium oxide from LakeShore. Ge 100 and Ge 1000 are Cryocal germanium thermometers [45].

see Fig. 9.6 which reports the transversal magnetoresistance of a Ge thermometer. Measurements of magnetoresistance down to 0.1 K are reported in ref. [70,71]. According to theory [72], the exponent of the Mott's law changes, and T_0 becomes proportional to the magnetic field.

We shall discuss the dynamic behaviour of Ge thermistor in Chapter 15.

9.6.2.2 Carbon resistors

Ge resistors are specifically produced for low-temperature thermometry; carbon and RuO_2 resistors are commercial products for electronics. Pure carbon is not a semiconductor. The negative slope $R(T)$ is due to the production process which consists in pressing and sinterization of carbon particles with glue. The resulting resistance is probably determined by the contact resistance between the particles. The cost of the carbon resistor thermometer is very low. Manufacturers such as Speer, Allen–Bradley and Matsushita have produced in the past carbon resistors for many years. Most of firms have now ceased manufacture, although their products may still be found in the storerooms of research laboratories.

Another useful device is the carbon-glass thermometer (CGT) [73] usable between $\sim$1 K and room temperature where it loses sensitivity. A nice property of CGT is its insensitivity to large magnetic fields [74,3, p. 269]. CGT are commercially available,

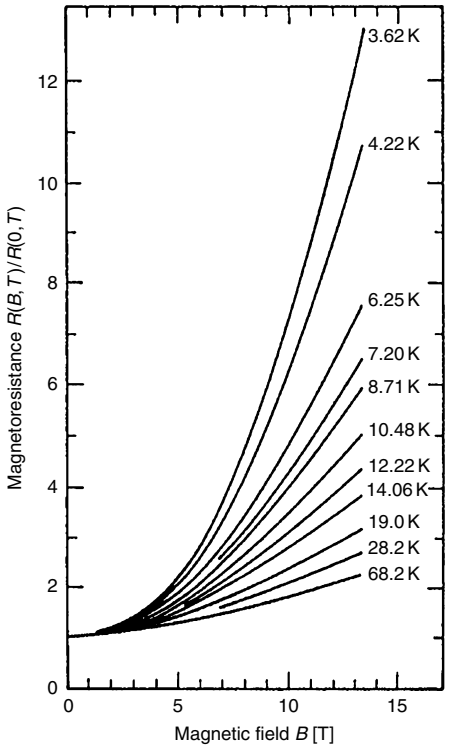

Fig. 9.6. Dependence on the magnetic field (perpendicular to current) of the electrical resistance of a Ge thermometer ($R_{4K} = 856\,\Omega$) at the indicated temperatures [68].

for example, from LakeShore and Cryotronics. As shown in Fig. 9.5, the $R(T)$ curve of CGT falls more steeply than carbon resistors, but eq. (9.14) can be used to represent their behaviour.

It must be noted (also for RuO_2 resistors) that resistors best suited for thermometry are those with the highest temperature coefficient, i.e. the worst for electronics (usually an high room temperature coefficient means also an high low-temperature coefficient). Of course, electronic firms tend to produce more stable resistors; hence the future will see the onset of an antiquary market for thermometers.

Detailed description of carbon resistor is found in some low-temperature text books [2,19,20]. Nowadays, they are usually replaced by thick-film resistors (RuO_2), which are also much easier to mount.

9.6.2.3 Thick-film RuO_2 resistors

RuO_2, zirconium oxinitride and metal oxide bead resistors are called oxide resistors.

RuO_2 resistors are commercial small-power (volume of few mm^3) electronic components. They belong to the group of smd (surface mount device) thick-film resistors and are

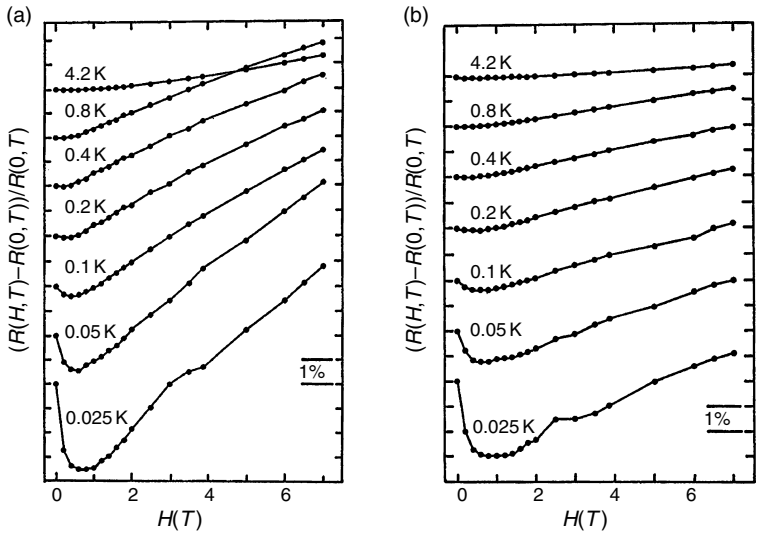

Fig. 9.7. (a) Magnetic field induced relative resistance change $(R(H, T)–R(0, T))/R(0, T)$ versus magnetic field for a 1 kΩ Dale RCW 575 resistor for seven different temperatures. The curves for each temperature are offset for clarity. (b) Magnetic field induced relative resistance change $(R(H, T)–R(0, T))/R(0, T)$ versus magnetic field for 2.7 kΩ Philips RC-01 resistor for seven different temperatures. The curves for each temperature are offset for clarity [78].

sold in wheels containing 2000–10 000 pieces for the automatized mounting of electronic circuits. The resistive material is a 'ceramic' consisting in a mixture of a component containing Ru and a Pb silicate, deposited onto an alumina support. The ratio between the two components defines the resistivity of the material. Below 1 K, the resistance of these thermometers follows approximately the Mott's law, with exponents ranging between 0.5 and 0.25 [75].

Small dimensions, easy mounting, good stability over thermal cycling and low cost are the qualities of these resistors. Magnetoresistivity is usually positive [76–78] for $T > 1$ K. For $T < 1$ K, both positive and negative values have been found (see Fig. 9.7) [78].

Due also to their (amorphous) composition, the heat capacity of a ruthenium oxide resistor is much higher than that of a Ge thermistor of equal mass [61]. This negative property prevents the use of RuO_2 resistors as detector sensors (see Chapter 15).

Note that the electronic industry produces smd components called 'thin-film resistors' of the same shape and size of RuO_2 thermistors. They are usually made of a thin layer of Ni-Cr. Their resistance is extremely stable with temperature and hence they find application as inexpensive (punctual) heaters (see e.g. Chapter 11).

9.6.2.4 Zirconium oxinitride

Zirconium oxinitride resistors (best known are Cernox) are thin-film resistors. Typical commercial sensors have resistance values of about $10^5\,\Omega$ at 1 K falling to $\sim 100\,\Omega$ at

100 K. Their useful range is from about 0.3 to 300 K. The stability is a few mK at 4 K. For more information about Cernox stability see ref. [79].

The magnetoresistance is less than 0.3% above 10 K; at 4.2 K a field of 13 T has a 2% effect (see ref. [80,81]. About 5000 cernox thermometers have been used at CERN for the control of Large Hadron Collider (LHC) [82].

Another commercial thermistor, Thermox (by LakeShore), is useful between 77 K (~80 kΩ) and room temperature (~0.3 Ω). It consists of a glass-encapsulated metal oxide bead. The short-term stability is about 25 mK in the useful range.

9.6.2.5 Junction diodes

Junction diodes are not strictly resistance thermometers but two terminal devices which are used in a similar way. The forward voltage drop is measured across a p–n junction carrying a constant d.c. of a few μA. Such voltage increases as the temperature falls. Junction diodes are Si, GaAs or AlGaAs commercial electronic components. They can be used above 1 K, but the voltage is almost linear above ~20 K. Typical sensitivities for Si diodes are 30 mV/K at 4 K and 2 mV/K at 77 K. Overheating (see Section 9.6.3) at low temperature is strong in this type of device. GaAs devices are less sensitive to both temperature and magnetic fields [[3], p.269]. The use of junction diodes for low-temperature thermometry has been reviewed in ref. [83,84].

9.6.3 Traps in resistance thermometry

Low-temperature resistance measurements do not differ in principle from room temperature ones: they can be carried out both in d.c. (carachteristographers) or in a.c. (bridges).

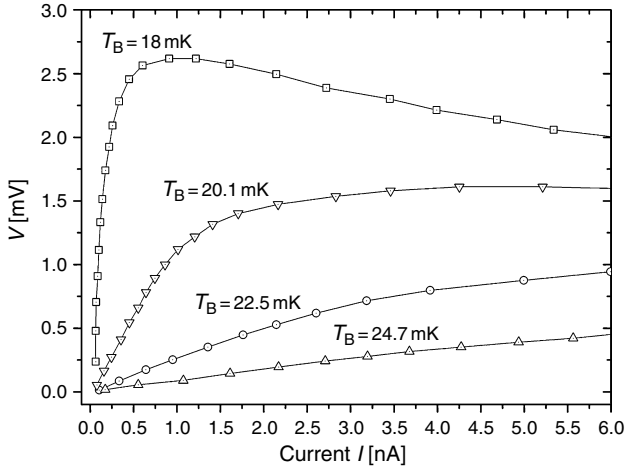

Fig. 9.8. *I–V* curve for a Ge-NTD#31 (see Section 15.2.1.1) resistor at four different temperatures T_B of the mixing chamber. Note the strong nonlinearity at low temperature.

Carachteristographers are d.c. instruments made up by a current (voltage) power supply and a voltage (current) meter. They give a two quadrant V–I relation for the resistive device. The information supplied by such instruments is more exhaustive than that supplied by a.c. bridges, but the measurement is time consuming, and an inversion of polarity is necessary to detect the possible presence of partially rectifying contacts. In Fig. 9.8, an example of a V–I relation in the first quadrant for a Ge-NTD#12 resistor (see Section 15.2.1.1) is shown. Note that the power used in the measurements can be as low as 10^{-14} W.

Bridges give a mean resistance value around $I = 0$. Strictly, they should be used only for linear components. In both cases (d.c. or a.c.), the resistance measurements are made in four-wire configuration, since the resistor to be measured is at low temperature whereas the measuring instrument is at room temperature: the electric connection is usually made by low thermal conductivity wires which are also poor electrical conductors (remind the Wiedeman–Franz law).

The power which must be supplied to the thermistor to measure its resistance depends on the noise level and on the detection system. The latter is the main responsible for the total noise (a few nV/$\sqrt{\text{Hz}}$), since the resistors are at low temperature and, hence, their thermal noise can be usually neglected (see eq. (9.17)).

The frequency response of the detection system is of low-pass type for characteristographers and band-pass for bridges (see Section 10.4). In both types of measurements the narrowing of the bandwidth corresponds to a longer time of measurement. Depending on the chosen detection system, several problems (true traps) may be encountered in resistance thermometry.

The main ones are:

1. Thermistor overheating

The small power needed to measure the resistance of the thermometer brings the thermometer at a temperature over that of the support surface. Such 'overheating' is due to the contact resistance at the interface (see Chapter 4). A typical value of the contact resistance is:

$$R_C \cdot T^3 = 8 \times 10^4 \ \left[\text{K}^2\text{m}^2/\text{W}\right] \tag{9.15}$$

For example, if we want a thermometer overheating $\Delta T/T$ less than 1%, with a contact surface $A = 10^{-4}\,\text{m}^2$, the power $P(T)$ to be supplied to the thermistor must be:

$$P(T) \leq T^4 \cdot 10^{-4}\,\text{W} \tag{9.16}$$

i.e. at 20 mK $P_{20\,\text{mK}} \leq 2 \times 10^{-11}$ W. With a typical value of resistance of 80 kΩ, the corresponding current is 15 nA.

Equation (9.15) is sometimes optimistic. Thermometer overheating as a function of temperature and contact resistance can be experimentally found, varying the power supplied to the thermometer while keeping constant the support temperature. This is shown in Fig. 9.9 for an RuO_2 thermometer. Note that a measuring power of 5×10^{-12} W at 20 mK produces an overheating of 12 mK!

The contact resistance may change when the thermometer is moved from a position to another. Hence the accuracy of resistance temperature measurements below about 25 mK

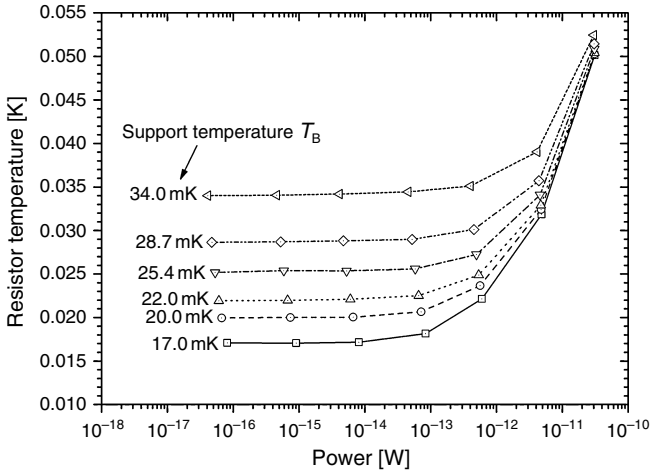

Fig. 9.9. Overheating of an RuO_2 thermometer as a function of temperature for six different support temperatures.

can be illusory. Moreover, in a.c. measurements of high-value resistances (more than 100 kΩ), another phenomenon may be present: since the measuring signal is d.c. coupled to the resistor, a current offset may be present in the output stage of the bridge. This is a random slow varying d.c. signal which supplies a small unpredictable additional power on the thermometer. An 1% current offset produces a 2% power offset. Also for this reason, the use of a secondary resistance thermometer driven with a.c. signal is not advisable below about 25 mK.

Last, we wish to remind that thermal cycling may spoil the thermometer calibration. The frequent check of the calibration by means of reference fixed points (see Section 8.5) is advisable.

2. Filtering

The four lines which electrically connect a thermometer at low temperature with the bridge at room temperature are usually filtered in order to reduce the interference of external noise sources. A low-pass filter may attenuate the signal detected by the bridge, thus giving an erroneous reading of the resistance. As example, let us simply schematize the filter with a capacitance $C = 10^{-8}$ F in parallel with the thermometer resistance R. If the bridge supplies a sinusoidal signal at 16 Hz (e.g. LR700 bridge.) and $R = 10^5\ \Omega$, the error due to the RC filter is $\Delta R/R = 5 \times 10^{-3}$. If $R = 5 \times 10^5\ \Omega$, $\Delta R/R = 12\%$. The situation is much more critical in the case of a square wave signal (e.g. Picowatt) or at higher frequencies. From this simplified example, we see that resistors of more than about 100 kΩ are to be usually avoided when working with a.c. bridges.

A suggestion: calibrate at room temperature your a.c. bridge connected to your filtered lines using resistors of increasing values to detect the real cut-off frequency of your apparatus.

9.7 Noise thermometry

The noise thermometer is based on the temperature dependence of the mean square noise voltage V^2 developed in a thermistor (Nyquist theorem, 1928):

$$V^2 = 4 \cdot k_B T \cdot R \cdot B \tag{9.17}$$

where B is the amplifier bandwidth.

The main problem encountered in low-temperature noise thermometry is the very low level of signals. For example, with $R = 1\,\mathrm{k\Omega}$ and $B = 1\,\mathrm{kHz}$:

- at 4 K, $V \approx 10^{-8}$ volt and $P = 10^{-19}\,\mathrm{W}$;
- at 10 mK, $V \approx 10^{-9}$ volt and $P = 10^{-22}\,\mathrm{W}$.

The latter values are not measurable by means of semiconductor amplifiers and a SQUID system is necessary.

Theoretically, the noise thermometer is a primary thermometer and as such has been used [85,86]. In practice, besides the low level of the signals to be detected, there are other problems [87,88], such as:

(a) noise generated by the resistive elements of the amplification devices;
(b) definition of the bandwidth B of the electronics;
(c) knowledge of the gain $A(f)$ of the electronics.

An additional drawback of this type of thermometry is the very long time needed for the measurement (more than 1 h for an 0.1% accuracy).

In the past, except for the low-temperature range, the uncertainties of noise thermometry were not comparable to those of the gas thermometry due to the non-ideal performance of detection electronics. Up to now, the most successful technique is the switched input digital correlator proposed by Brixy et al. in 1992 [89]. In this method, the noise voltage is fed via two separate pairs of leads to two identical amplifiers whose output signals are multiplied together, squared and time averaged (see Fig. 9.10).

This eliminates the amplifier and transmission line noise superimposed on the thermal noise, since the respective noise voltages are uncorrelated.

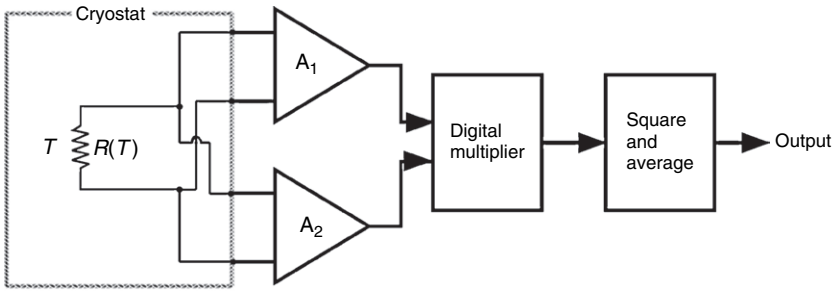

Fig. 9.10. Block diagram of the switched input digital correlator.

The possibility of using the Brixy technique for low-temperature thermometry is under study (see e.g. ref. [90]).

9.8 Dielectric constant thermometry

Capacitance measurements are quite simple. A typical drawback is the need of coaxial cables that introduce a thermal load which is not negligible in low-power refrigerators. On the other hand, capacitance bridges null the cable capacitance. Multiplexing is more difficult than for resistance thermometers. In principle, capacitors have low loss due to Joule heating. This is not always true: losses can be important, especially at very low temperatures. Dielectric constant thermometers have a high sensitivity: capacitance differences of the order of 10^{-19} F can be measured.

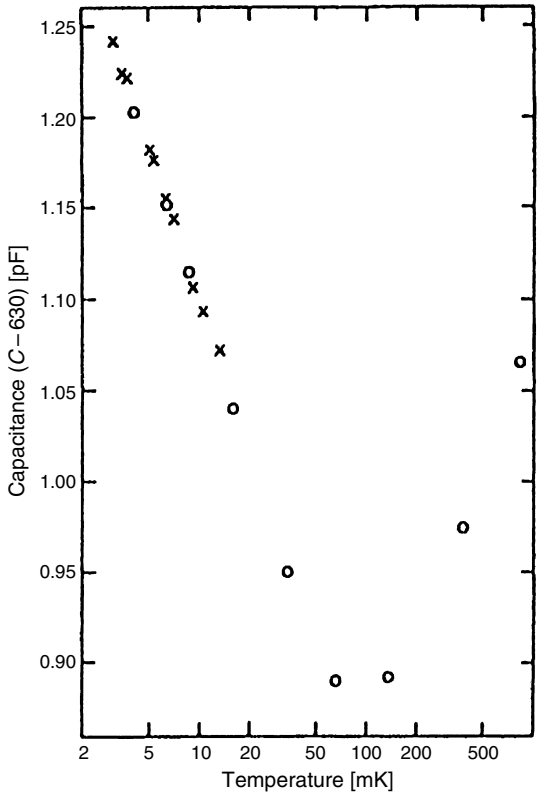

Fig. 9.11. Capacitance (minus 630 pF) of a capacitive glass thermometer as a function of temperature. The data points were obtained at excitation frequencies of 1.0 and 4.7 kHz at zero magnetic field (x) and at $B = 9$ T (o) [92].

Several materials show an appreciable temperature dependence of the dielectric constant down to a few millikelvin. In Fig. 9.11, such dependence is shown for a glass (SiO_2 with 1200 ppm of OH^- [91,92]). Note the presence of a minimum which usually depends on the measuring frequency.

An interesting aspect of dielectric constant thermometry is the small influence of a magnetic field. On the other hand, measurements depend on both the measuring frequency and voltage (see Figs 9.12 and 9.13). Figure 9.13 shows an example of the dependence on frequency of both the dielectric constant and loss for Upilex S [93].

Figure 9.14 shows the low-temperature dependence of the dielectric constant for an epoxy (Emerson & Cuming, Stycast 1266) [94].

Many commercial capacitors can be used as thermometers since they show a strong dependence of their capacitance on temperature. Figure 9.15 shows the low-temperature $C(T)$ curve for a commercial smd capacitor (ceramic capacitor KEMET-Y5V).

Above the minimum, the mean slope of $C(T)$ is about 0.6 pF/mK up to room temperature. Such commercial capacitor would be a thermometer with a very large operating range, a property not very common in other thermometers.

Unfortunately, most capacitance thermometers are not stable and must be recalibrated at every cool down. They may also present problems of 'heat release' [95]: moreover, their thermalization times at low temperatures may be long since the materials used present low thermal conductivity and high specific heat.

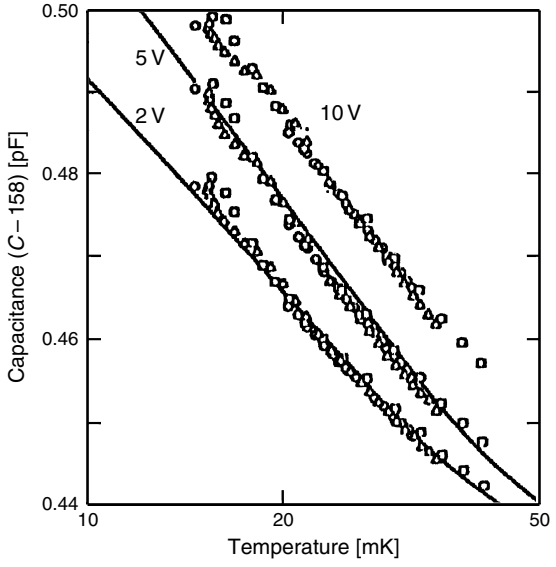

Fig. 9.12. Capacitance of a capacitive glass thermometer as a function of temperature at the same frequency (4.7 kHz) for three measuring voltages. The measurements were carried out in magnetic field of: 0.0 T (∘), 0.25 T (Δ) and 6.0 T (□) [91].

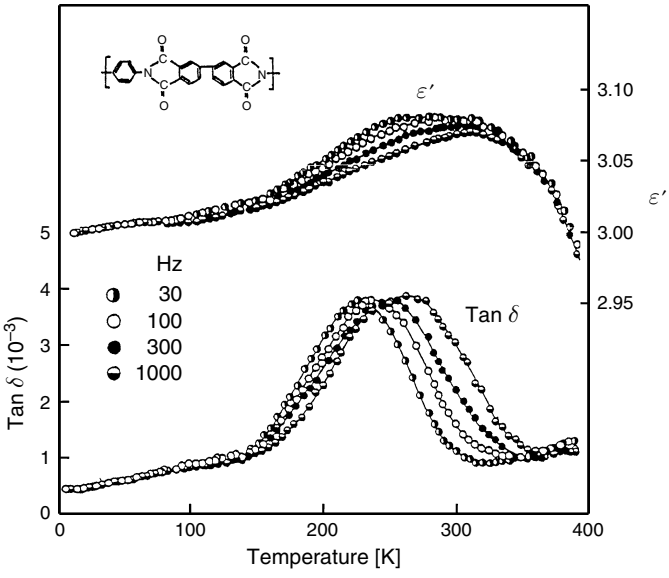

Fig. 9.13. Dielectric properties of Upilex-S as a function of temperature at four measurement frequencies [93].

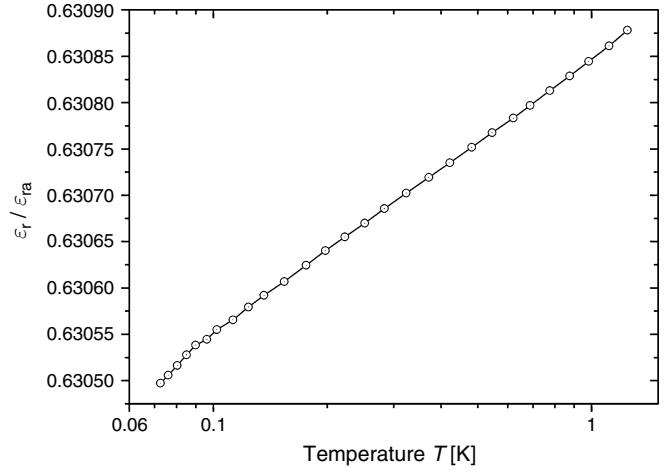

Fig. 9.14. Temperature dependence of the dielectric constant ε_r of Stycast 1266 below 1 K. ε_{ra} is the dielectric constant in vacuum at room temperature [94].

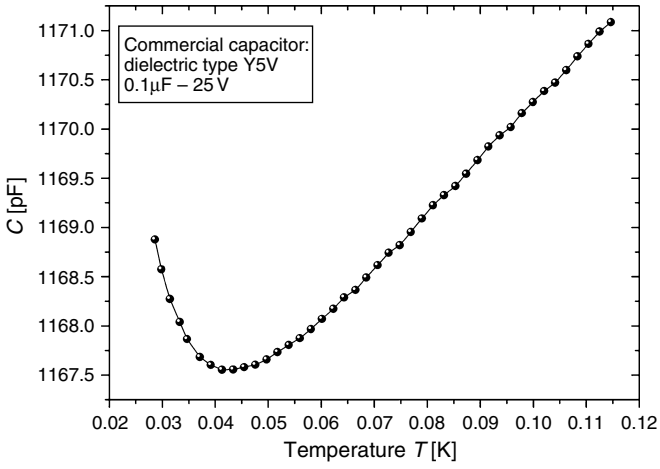

Fig. 9.15. Capacitance of an smd capacitor (ceramic capacitor KEMET-Y5V) as a function of temperature.

9.9 Paramagnetic salt thermometry

The starting relation is the Curie–Weiss law:

$$\chi = \chi_0 + \frac{\lambda}{T - \Delta} \tag{9.18}$$

where χ is magnetic susceptibility of the paramagnetic material and λ is the Curie constant. The Weiss constant Δ depends on the shape of the thermometric sample, on the crystal symmetry and on the interaction between the magnetic moments. Since the parameters of the Curie–Weiss relation (9.18) cannot be defined theoretically, a calibration of the thermometer is necessary. Hence, this is a secondary thermometer.

The paramagnetic salts useful for this type of thermometry are the same as that used in the ADR (adiabatic demagnetization refrigerator, see Section 7.3 and Fig. 7.7). The most commonly used salts are:

- MAS: $(Mn^{2+}\ SO_4 \cdot (NH_4)_2\ SO_4 \cdot 8H_2O)$, $T_c \sim 0.17\,K$;
- FAA: $(Fe^{3+}\ (SO_4)_3 \cdot (NH_4)_2SO_4 \cdot 24H_2O)$, $T_c \sim 0.03\,K$;
- CPA: $(Cr_2^{3+}(SO_4)_3 \cdot K_2SO_4 24H_2O)$, $T_c \sim 0.01\,K$;
- CMN: $(2Ce^{3+}(NO_3)_3 \cdot 3Mg(NO_3)_2 \cdot 24\ H_2O)$, $T_c \sim 0.002\,K$.

where T_c is the minimum temperature usable for each salt.

Note that CMN is the best suited salt for very low-temperature thermometry. The value of T_c can be further decreased to 0.2 mK, partly substituting ions Ce^{3+} with ions La^{3+}.

All these salts contain crystallization water which assure a large distance (about 1 nm on CMN) among the magnetic ions giving a low T_c [1].

We wish to remind that these salts cannot be kept under vacuum at room temperature since they lose the crystallization water.

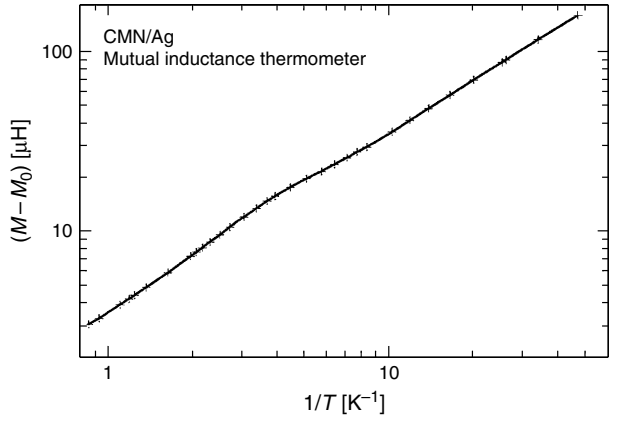

Fig. 9.16. Mutual inductance M (minus electrical connection contribution M_0) versus $1/T$ for a CMN thermometer.

For this type of thermometry a mutual inductance meter of high sensitivity (10^{-9} H) is needed.

Deviations from the $1/T$ dependence are generally observed; these are due to magnetic parasitic contributions (see example of Fig. 9.16 where M_0 is the mutual inductance of the electrical connections).

9.10 Nuclear orientation thermometry

In this type of thermometry, long mean-life radioactive nuclei are used. The latter perform a $\beta^{\pm}$ decay into an excited state which emits γ to return to the fundamental state as depicted in Fig. 9.17.

If radioactive nuclei (^{60}Co and ^{54}Mn are commonly used) are polarized by a strong magnetic field, the direction of emitted γ rays is anisotropic: the emission probability is a function of the angle with the field. Such angular distribution depends on the $(2I+1)$ levels of the nuclear spin in the local magnetic field and is a function of temperature T. In fact, the relative population of such levels is determined by the Boltzmann factor $\exp(-\beta_m \Delta_{\mathrm{hf}})$, with $\beta = 1/k_{\mathrm{B}}T$, m the I component along the local field and Δ_{hf} the hyperfine splitting between two adjacent levels. For $T >> \Delta_{\mathrm{hf}}/k_{\mathrm{B}}$ all levels are equally populated; hence, the γ emission is isotropic; for $T << \Delta_{\mathrm{hf}}/k_{\mathrm{B}}$ only the fundamental level is occupied, hence the anisotropy is practically not dependent on temperature.

There is, however, a temperature range in which the γ emission is a function of temperature. In this range, the anisotropy of γ emission can be used as thermometric property. The advantage of using γ emitters is that the detection can be done from outside the cryostat (no wiring necessary inside the cryostat).

Figure 9.18 shows, for ^{60}Co, the $W(\theta, T)$ function, i.e. the ratio of γ ray intensity for an angle θ with the field direction and the 'isotropic' intensity. On a smaller scale, also the

sensitivity $dW/d\theta$, which has a maximum for $\theta = 90°$, is shown: the useful temperature range is about 2–60 mK.

Since an appreciable polarization of nuclear magnetic moments requires high fields ($10 \div 30$ T), ^{60}Co or ^{54}Mn atoms are embedded in ferromagnetic crystals (usually Fe, Ni or ^{59}Co) to get the same local field for all nuclei. However, since also the magnetic

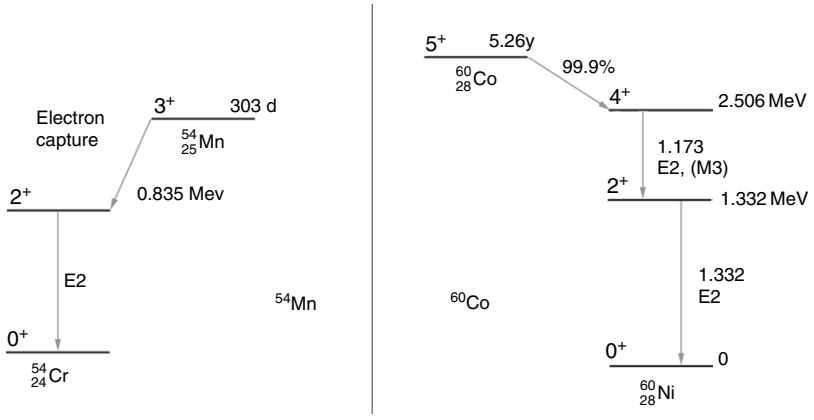

Fig. 9.17. Energy level diagrams for ^{54}Mn and ^{60}Co (slightly simplified). These are the two decay favourite schemes used for nuclear orientation thermometry.

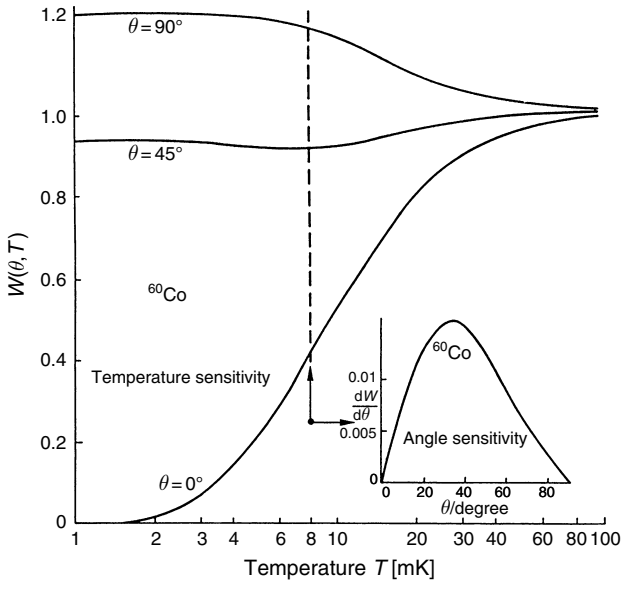

Fig. 9.18. $W(\theta, T)$ function for ^{60}Co (see text) [96].

domains must be aligned, an external field of $0.1 \div 1$ T is applied; in calculations also, this external field must be taken into account. The radioactive atoms are usually introduced into the crystal by a surface deposition followed by high-temperature diffusion; ^{60}Co may be otherwise produced by neutron irradiation of ^{59}Co.

A significant source of error in nuclear orientation thermometers is due to the possible absorption of the radioactive emission in the cryostat, with a temperature increase; as a consequence, low-intensity source must be used, with long counting periods to get a good statistics.

Typical power values released by the radioactive substances used in nuclear orientation thermometers are:

- 1 μCurie ^{60}Co: 0.57 nW due to β emission;
- 1 μCurie ^{54}Mn: 0.03 nW due to 5 keV peak of ^{54}Cr after electron capture [97–105].

A drawback of nuclear orientation thermometry is the narrow range where the sensitivity $T(\mathrm{d}W/\mathrm{d}T)$ is adequate for measurements; it happens around $T \approx \Delta_{hf}/k_B$ (see Figs 9.18 and 9.19). $\Delta_{hf}/k_B = 9.14$ mK for ^{54}Mn in Fe and $\Delta_{hf}/k_B = 7.965$ mK for ^{60}Co in Fe. Moreover, since the statistic error on the measurement is $\Delta T/T = (2/n)^{1/2}$ (for n counts), long counting times, typically 10^3 s, but potentially up to 10^5 s for 1% precision at the lowest temperatures, are needed. The temperature should be stable over these timescales.

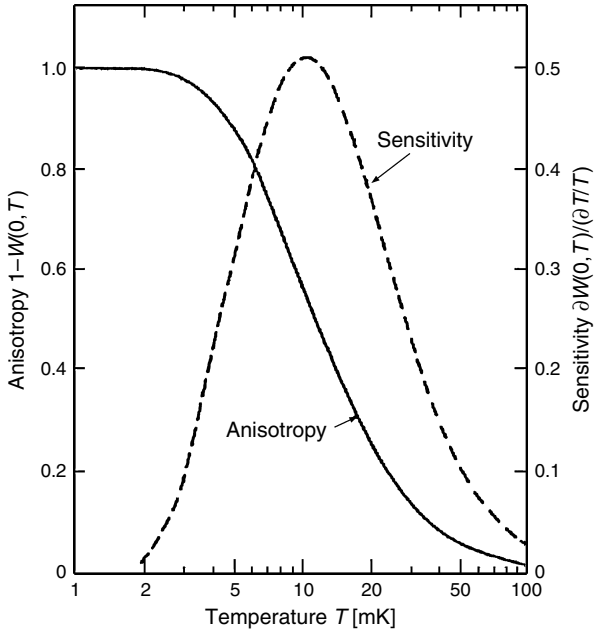

Fig. 9.19. Temperature dependence of the anisotropy of the γ radiation of ^{54}Mn in Ni host along $\theta = 0$. The quantity $\partial W/\partial T$ is a measure of the temperature sensitivity of the thermometer which, in this case, has its maximum value at about 10 mK [1].

An advantage of this technique, instead, is the good thermal contact with the (metallic) radioactive material, and, more important, the good thermal coupling between lattice and nuclear spins. Last, the γ ray energy is usually quite high, and no special window in the cryostat is needed. Nuclear orientation thermometer is a primary thermometer.

Comparisons among various thermometers and the nuclear orientation thermometer can be found in ref. [100–105] Further information may be obtained from ref. [97,106,107].

9.11 Magnetic thermometry with nuclear paramagnets

The low-temperature limit of magnetic thermometry with paramagnetic salts (see Section 9.9) is given by the ordering temperature of the electronic magnetic moments. Such ordering temperature is around 1 mK (example the CMN thermometer).

For a lower temperature thermometry, one has to move from electronic paramagnets to nuclear paramagnets. Magnetic thermometry with nuclear paramagnets extends the range of thermometry down to a few microkelvin.

Since the magnetic moments are smaller, now we have a smaller susceptibility and therefore much smaller signal, requiring more sensitive detection systems. These are resonance or SQUID (see Section 14.5) techniques. Thermal response time are shorter, since pure metals can be used with good thermal conductivity and fast spin-lattice relaxation. The parameter to be measured is the nuclear susceptibility:

$$\chi_n = \frac{\lambda_n}{T_n} \tag{9.19}$$

with:

$$\lambda_n = \frac{N_0 I \cdot (I+1)\, \mu_0 \mu_n^2 g_n^2}{3k_B} \tag{9.20}$$

In many metals, this law (Curie law) should be valid for at least few μK. For example, for Cu and Pt, it seems to be true with a 1% confidence for fields below 1 mT [2].

Nevertheless deviations from eq. (9.19) have been observed for the intermetallic compound $AuIn_2$ [108,109] and for Tl [110,111]. Requirements for the validity of eq. (9.19) are the absence of changing internal fields due to nuclear magnetic or electronic magnetic ordering in the relevant temperature range, the absence of nuclear electronic quadrupole interactions and no superconductive transition.

Nuclear magnetic thermometry is fundamental for the microkelvin range, but at higher temperatures the signal can be rather weak and may be overcome by contributions from electronic magnetic impurities. For the methods of detection of nuclear magnetization, see e.g. ref. [2].

9.12 Coulomb blockade thermometry

Coulomb blockade thermometry (CBT) is based on the electric conductance characteristics of tunnel junctions. This type of thermometer has been developed at Jyväskylä University. The basic results are reported in ref. [112].

The conductance of a tunnel junction array is determined by three energy contributions: the thermal energy $k_B T$, the electric potential energy eV at bias voltage V and the charging energy $\varepsilon_c = e^2/2C_{eff}$, where C_{eff} is the effective capacitance of the array and $\varepsilon_c = [(N-1)/N]e^2/C$ with N the number of junctions in series.

If $k_B T >> \varepsilon_c$, the dynamic conductance of a junction array is given by [111]:

$$\frac{G}{G_T} = 1 - \left(\frac{\varepsilon_c}{k_B T}\right) \cdot g\left(\frac{eV}{Nk_B T}\right) \tag{9.21}$$

where G_T is the asymptotic conductance at high bias voltage. The function g, which is nearly Gaussian shaped around zero, is given by:

$$g(x) = \frac{\left[x \cdot \sinh(x) - 4\sinh^2(x/2)\right]}{8\sinh^4(x/2)} \tag{9.22}$$

The full width at half minimum of the conductance dip described by eq. (9.21) (see Fig. 9.20) is proportional to the temperature T.

The useful temperature range of CBT is defined by the number and size of the tunnel junctions. These are realized by vacuum evaporation of ~100 nm Al layers (which are

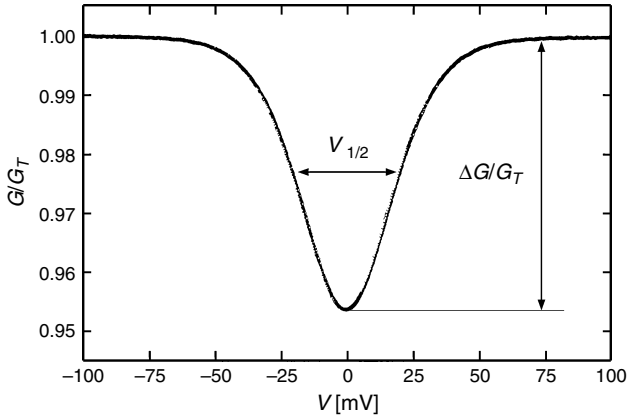

Fig. 9.20. Normalized conductance G/G_T of a coulomb blockade thermometry sensor versus bias voltage V.

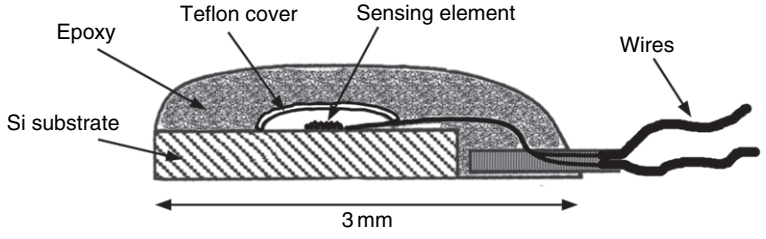

Fig. 9.21. Scheme of a sensor for Coulomb blockade thermometry.

successively oxidized) and ∼200 nm of Cu. The substrate is Si oxide. Junctions have a surface of $\sim 1.5\,\mu m^2$. A scheme of the sensor is shown in Fig. 9.21.

The useful range of CBT is $0.02 \div 10\,K$ [113]. For temperatures below ∼1.18 K, a week magnetic field ($0.1 \div 0.2\,T$) must be applied to the sensor to suppress Al superconductivity. For temperatures below ∼20 mK, electron–phonon decoupling is present. CBT is useful when working with high magnetic fields. The sensor in fact shows a negligible magnetoresistance: tests in the $0.05 \div 4.2\,K$ temperature range and with field up to 31 T have been performed [114].

The CBT is in principle a primary thermometer, but its absolute accuracy is at present too low for metrological applications [115].

References

[1] O.V. Lounasmaa: *Experimental Principles and Methods Below 1 K*, Academic, London (1974)
[2] F. Pobell: *Matter and Methods at Low Temperatures*, Springer, Berlin (1995)
[3] T. Quinn: *Temperature*, Academic Press, London (1990)
[4] R.E. Bentley: *Theory and Practice of Thermoelectric Thermometry*, Springer Verlag, Singapore (1998)
[5] L.G. Rubin: Cryogenics **10**, 14 (1970)
[6] L.G. Rubin, B.L. Brandt, H.H. Sample: Cryogenics **22**, 491 (1982)
[7] L.G. Rubin: Cryogenics **37**, 341 (1997)
[8] G. Schuster, D. Hechtfisher, B. Fellmutt: Rep. Prog. Phys. **57**, 187 (1994)
[9] R.C. Kemp, W.R.G. Kemp, L. Besley: Metrologia **23**, 61 (1987)
[10] G.T. McConville: *Proc. LT-17*, p. 401, Elsevier Science (1984)
[11] F.C. Matacottaer et al.: Jpn. J. Appl. Phys. **26**, 1679 (1987)
[12] F.C. Matacotta et al.: Metrologia **24**, 61 (1987)
[13] P.P.M. Steur, M. Duriex, G.T. McConville: Metrologia **24**, 69 (1987)
[14] R.A. Aziz, M.J. Slaman: Metrologia **27**, 211 (1990)
[15] F. Pavese, G. Molinar: *Modern Gas-Based Temperature and Pressure Measurements*, Plenum Press, New York and London (1992)
[16] K.D. Hill: Metrologia 39, 41 (2004)
[17] D.N. Astrov et al.: Metrologia, **26**, 151 (1989)
[18] P.P.M. Steur, M. Durieux: Metrologia **23**, 1 (1986)
[19] G.K. White: *Experimental Techniques in Low-Temperature Physics*, Clarendon, Oxford (1979)
[20] A.C. Rose-Innes: *Low-Temperature Laboratory Techniques*, English University Press, London (1973)
[21] T.J. Quinn: Physica Scripta 41,730 (1990)
[22] P.P.M. Steur: Jpn. J. Appl. Phys. **26**, 1685 (1987)
[23] P.P.M. Steur and F. Pavese: Cryogenics **29**, 135 (1989)
[24] Y. Iye: Cryogenics **28**, 164 (1988)
[25] K. Nara, R.L. Rusby, D.I. Head: Cryogenics **30**, 952 (1990)
[26] H. Sakurai: *Temperature: Its Measurement and Control in Science and Industry*, vol. 6, p. 127, ed. by J.F. Schooley, American Institute of Physics, New York (1992)
[27] K. Grohmann, H. Kock: Proc. LT 17, eds. U. Eckern, A. Schmid, W. Weber, and H. Wuhl, Elsevier Press, Amsterdam (1984)
[28] K.S. Izrailov, R.E. Taimonov: Meas. Tech. **28**, 857 (1985)
[29] D. Gugan, G.W. Michel: Metrologia **16**, 149 (1980)
[30] D. Guganl: Metrologia **28**, 405 (1991)
[31] K. Grohmann, H. Luther: *Temperature: Its Measurement and Control in Science and Industry*, vol. 6, p. 21, ed. by J.F. Schooley, American Institute of Physics, New York (1992)
[32] M.R. Moldover, J.P.M. Trussler: Metrlogia **25**, 165 (1988)
[33] M.R. Moldover et al.: J. Res. Natl. Bur. Stand. **104**, 11 (1999)

[34] B.W. Petley: *Phys. Scr.* **T40**, 5 (1992)
[35] W. Cencek, K. Szalewicz, B. Jeziorski: Phys. Rev. Lett. **86**, 5675 (2001)
[36] G. Lach, B. Jeziorski, K. Szalewicz: Phys. Rev. Lett. **92**, 233001 (2004)
[37] D.Gugan, G.W. Michel: Metrologia **16**, 149 (1980)
[38] H. Luther, K. Grohmann, B. Fellmuth: Metrologia **33**, 341 (1996)
[39] B. Fellmuth et al.: *Dielectric-Constant Gas Thermometry and Determination of the Boltzmann Constant* TEMP-MEKO 2004, Cavtat–Dubrovnik Croatia, ISBN number 953-6313-73-1
[40] E.F. May et al.: Rev. Sci. Instrum. **75**, 3307 (2004)
[41] R.T. Jacobsen, S.G. Penoncello, E.W. Lemmon: *Thermodynamic Properties of Cryogenic fluids*, Plenum Press, New York (1996)
[42] H. Preston-Thomas: Metrologia **27**, 3 (1990)
[43] B.W. Magnum: J. Res. NIST **95**, 69 (1990)
[44] BIPM *Techniques for Approximating the International Temperature Scale of 1990*, Bureau International des Poids et Mesures, Sevres (1990)
[45] G.K. White, P.J. Meeson: *Experimental Techniques in Low-Temperature Physics*, 4th ed., Clarendon Press, Oxford (2002)
[46] V. Steinberg, G. Ahlers: J. Low Temp. Phys. **53**, 255 (1983)
[47] D.S. Greywall, P.A. Bush: Rev. Sci. Instrum. **51**, 509 (1980)
[48] W.P. Halperin et al.: J. Low Temp. Phys. **31**, 617 (1978)
[49] E.R. Grilly: J. Low Temp. Phys. **11**, 243 (1973)
[50] M. Barucci et al.: Cryogenics **40**, 437 (2000)
[51] D.S. Greywall: Phys. Rev. B **31**, 2675 (1985)
[52] R.A. Scribner, E.D. Adams: in *Temperature, Its Measurement and Control in Science and Industry*, vol. 4, p. 37, ed. by H.H. Plumb, Instrument Society of America, Pittsburgh, PA (1972)
[53] J.R. Thompson, H. Meyer: Cryogenics **7**, 296 (1967)
[54] G.C. Straty, E.D. Adams: Rev. Sci. Instrum. **40**, 1393 (1969)
[55] W.P. Halperin et al.: Phys. Rev. Lett. **34**, 718 (1975)
[56] R.J. Soulen, Jr., W.E. Fogle, J.H. Colwell: J. Low Temp. Phys. **94**, 385 (1994)
[57] W.E. Fogle, R.J. Soulen Jr., J.H. Colwell: in *Temperature: Its Measurement and Control in Science and Industry*, vol. 6, p. 91, ed. by J.F. Schooley, American Institute of Physics, New York (1992)
[58] R.J. Soulen, Jr: Physica B **109&110**, 2020 (1982)
[59] G. Schuster, A. Hoffmann, D. Hechtfischer: Czech. J. Phys. **46**, 481 (1996)
[60] D.S. Greywall, P.A. Busch: J. Low Temp. Phys. **46**, 451 (1982)
[61] G. Schuster et al.: Physica B **165&166**, 31 (1990)
[62] G. Frossati: J. Physique **41** (C7), 95 (1980)
[63] C.C. Kranenburg et al.: Jpn. J. Appl. Phys. **26**, 215 (1987)
[64] D.J. Bradley et al.: J. Low Temp. Phys. **45**, 357 (1981)
[65] N.F. Mott: Phil. Mag. **19**, 835 (1969)
[66] B.I. Shklovskii: Phys Rev B **67**(4), 045201 (2003)
[67] D. McCammon et al.: NIM A **436**, 205 (1999)
[68] L.J. Neuringer et al.: Rev. Sci. Instrum. **42**, 9 (1971)
[69] H.H. Sample, L.G. Rubin: Cryogenics **17**, 597 (1977)
[70] P. De Moor et al.: J.Appl.Phys. **79**, 3811 (1996)
[71] E. Pasca et al.: *Bolometers in Magnetic field: Use of NTD Ge Sensors*, NIM A 2007 in print, available online: http://dx.doi.org/10.1016/j.nima.2007.02.092
[72] B.I. Shklovskii, A.L. Efros: *Electronic Properties of Doped Semiconductors*, Springer, Berlin (1984)
[73] W.N. Lawless: Rev. Sci. Instrum. **43**, 1743 (1972)
[74] L.G. Rubin, B.L. Brandt: Adv. Cryogenic. Eng. **31**, 1221 (1986)
[75] A. Briggs: Cryogenics **31**, 932 (1991)
[76] W.A. Bosh et al.: Cryogenics **26**, 3 (1986)
[77] M.L. Sigueira, R.J. Viana, R.E. Rapp: Cryogenics **31**, 796 (1991)
[78] K. Uhlig: Cryogenics **35**, 525 (1995)
[79] D. Giraudi et al.: *Proc. of TEMP-MEKO 1996*, ed. by P.Marcarino, p.155, Levrotto and Bella, Turin (1997)

[80] G. Heine, W. Lang: Cryogenics **38**, 377 (1998)
[81] H.D. Ramsbotton, S. Ali, D.P. Hampshire: Cryogenics **36**, 61 (1996)
[82] T. Junquera et al.: *Neutron Irradiation Tests of Calibrated Cryogenic Sensors on Low Temperatures*, CERN-LHC Project Report n°153 (1997)
[83] J.K. Krause, P.R. Swinehart: Adv. Cryog. Eng. **31**, 1247 (1986)
[84] M.G. Rao, R.G. Scurlock, Y.Y. Wu: Cryogenics **23**, 635 (1983)
[85] R.P. Giffard, R.A. Webb, J.C. Wheatley: J. Low Temp. **6**, 533 (1972)
[86] R.P. Giffard, R.A. Webb, J.C. Wheatley: J. Low Temp. **13**, 383 (1973)
[87] D.R. White et al.:Metrologia **33**, 325 (1996)
[88] L. Crovin, A. Actis: Metrologia **14**, 69 (1978)
[89] H. Brixy et al.: in *Temperature: Its Measurement and Control in Science and Industry*, vol. 6, p. 993, Toronto, ed. by J.F. Schooley, American Institute of Physics, New York (1992)
[90] H. Sakurai: in *Proc. of SICE Annual Conference in Fuhi*, p. 3029, Fukui University, Japan (2003)
[91] P.J. Reijntjis et al.: Rev. Sci. Instrum **57**, 1413 (1986)
[92] S.A.J. Wiegers et al.: Rev. Sci. Instrum. **58**, 2274 (1987)
[93] O. Yano, H. Yamaoka: Prog. Polym. Sci. **20**, 585 (1995)
[94] G. Ventura et al.: Cryogenics **39**, 963 (1999)
[95] K. Gloos et al.: J. Low Temp. Phys. **73**, 101 (1988)
[96] D.S. Betts: *Refigeration and Thermometry Below One Kelvin*, Sussex University Press, Brighton (1976)
[97] R.P. Hudson et al.: J. Low Temp. Phys. **20**, 1 (1975)
[98] D.S. Parker, L.R. Corruccini: Cryogenics **15**, 499 (1975)
[99] R.C. Richardson: Physica B **90**, 47 (1977)
[100] S.R. de Groot, H.A. Tolhoek, W.J. Huiskamp: *Alpha-, Beta-, and Gamma-Ray Spectroscopy*, vol. 2, p. 1199, ed. by K. Siegbahn, North-Holland, Amsterdam (1985)
[101] H.J. Rose, D.M. Brink: Rev. Mod. Phys. **39**, 306 (1967)
[102] H. Marshak: J. Low Temp. Phys. **6**, 769 (1972)
[103] P.M. Berglund et al.: J. Low Temp. Phys. **6**, 357 (1972)
[104] J.R. Sites, H.A. Smith, W.A. Steyert: J. Low Temp. Phys. **4**, 605 (1971)
[105] N.J. Stone, H. Postma eds.: *Low Temperature Nuclear Orientation*, North-Holland, Amsterdam (1986)
[106] R.J. Soulen Jr., H. Marshak: Cryogenics **20**, 408 (1980)
[107] G. Shuster, D. Hectfisher, B. Fellmuth: Rep. Prog. Phys. **57**, 187 (1994)
[108] T. Herrmannsdörfer et al.: Phys. Rev. Lett. **74**, 1665 (1995)
[109] T. Herrmannsdörfer, F. Pobell: J. Low Temp. Phys. **100**, 253 (1995)
[110] U. Angerer, G. Eska: Cryogenics **24**, 515 (1984)
[111] G. Eska, E. Schubert: Jpn. J. Appl. Phys., Suppl. **26(3)**, 435 (1987) (*Proc. 18th Int'l Conf. Low Temp. Phys.*)
[112] J.P. Pekola et al.: Phys. Rev. Lett. **73**, 2903 (1994)
[113] J.P. Pekola et al.: J. Low Temp. Phys. **128**, 263 (2002)
[114] J.P. Pekola et al.: J. Appl. Phys. **83**, 5582 (1998)
[115] A.J. Manninen et al.: Physica B **284–288**, 2010 (2000)